Articles

Subunit Interface Residues of Glutathione *S*-Transferase A1-1 that Are Important in the Monomer−Dimer Equilibrium†

Melissa A. Vargo, Lucia Nguyen, and Roberta F. Colman*

Department of Chemistry and Biochemistry, University of Delaware, Newark, Delaware 19716

Received November 26, 2003; Revised Manuscript Received January 9, 2004

ABSTRACT: Alpha class glutathione *S*-transferase, isozyme A1-1, is a dimer (51 kDa) of identical subunits. Using the crystal structure, two main areas of subunit interaction were chosen for study: (1) the hydrophobic ball and socket comprised of Phe52 from one subunit fitting into a socket formed on the other subunit by Met94, Phe136, and Val139 and (2) the Arg/Glu region consisting of Arg69 and Glu97 from both subunits. We introduced substitutions of these residues, by site-directed mutagenesis, to evaluate the importance of each at the subunit interface and to determine if monomeric enzymes could be generated using single mutations. Mutating each residue of the socket region to alanine results in little change in the kinetic parameters, and all are dimeric enzymes. In contrast, when Phe52, the ball residue, is replaced with alanine, the enzyme has very low activity and a weight average molecular mass of 31.9 kDa, as determined by sedimentation equilibrium experiments. Substitutions for Glu97 which eliminate the charge cause no appreciable changes in the kinetic parameters or molecular mass. Eliminating the charge on Arg69 (as in R69Q) results in a dimeric enzyme; however, when the charge is reversed (as in R69E), the weight average molecular mass is greatly shifted toward that of the monomer (33 kDa) and the changes in kinetic parameters are reasonably small. We determined the molecular masses in the presence of glutathione for F52A and R69E to ascertain whether the monomeric species retains activity. For R69E, it appears that the monomer is active, albeit less so than the dimer, while for F52A, the monomer and dimer both appear to exhibit very low activity. The dimeric species is needed to obtain high specific activity. We conclude that, of the residues that were studied, Phe52 and Arg69 are the major determinants of dimer formation and a single mutation at either position substantially hinders dimerization. The use of a mutant glutathione *S*-transferase which retains activity yet has a greatly weakened tendency to dimerize (such as R69E) may be advantageous for certain applications of GST fusion proteins.

Glutathione *S*-transferases (GSTs,[1] EC 2.5.1.18) constitute a family of detoxification enzymes that are involved in the metabolism of endogenous and xenobiotic compounds (*1*−*4*). All of these enzymes catalyze the conjugation of glutathione to the electrophilic center of a variety of substrates, resulting in a more water soluble product that can be further degraded or transported out of the cell. GSTs have been implicated in the development of anticancer drug resistance and have been found in elevated levels in tumors (*5*). The cytosolic enzymes are grouped into several classes based on their sequence homology and substrate specificities. There are crystal structures to represent most of the classes.

Isozyme 1-1 (A1-1),[2] a member of the alpha class, is the major isozyme found in the mammalian liver, making up ∼2% of the cytosolic protein (*6*). The unique features of the alpha class are a non-substrate steroid binding site (*7*, *8*), a C-terminal α-helix that closes over part of the hydrophobic binding site, and the efficiency with which it catalyzes the isomerization of Δ^5-androstene-3,17-dione to Δ^4-androstene-3,17-dione (*9*). The enzyme is crystallized as a homodimer with a molecular mass of 51 kDa. The N-terminal portion of one monomer interacts primarily with the C-terminal portion of the other subunit. Each subunit has a complete active site, including a glutathione binding site and a xenobiotic substrate binding site.

The crystal structure shows three main areas of interaction at the subunit interface (*10*), of which we chose two to study (Figure 1). The first area (Figure 1A) is predominantly hydrophobic, in which Phe52 from one monomer is wedged into a space created by several residues in the other subunit, some of which are Met94, Phe136, and Val139. This interaction is known as the hydrophobic ball and socket. Phe52 is 3.6 Å from the closest atom of Phe136 of the

† This work was funded by NIH Grant R01-CA66561 (R.F.C.) and by NIH Grant T32 GM-08550 (for M.A.V.).

* To whom correspondence should be addressed. Telephone: (302) 831-2973. Fax: (302) 831-6335. E-mail: rfcolman@chem.udel.edu.

[1] Abbreviations: GST, glutathione *S*-transferase; GSH, glutathione; CDNB, 1-chloro-2,4-dinitrobenzene; IPTG, isopropyl thio-β-D-galactopyranoside; Tris, tris(hydroxymethyl)aminomethane; Ni−NTA, nickel nitrilotriacetic acid; EDTA, ethylenediaminetetraacetic acid; SDS−PAGE, sodium dodecyl sulfate−polyacrylamide gel electrophoresis.

[2] Glutathione *S*-transferase, isozyme 1-1, is designated as the rGSTA1-1 isozyme in the nomenclature of Hayes and Pulford (*5*).

10.1021/bi030245z CCC: $27.50
Published on Web 03/05/2004

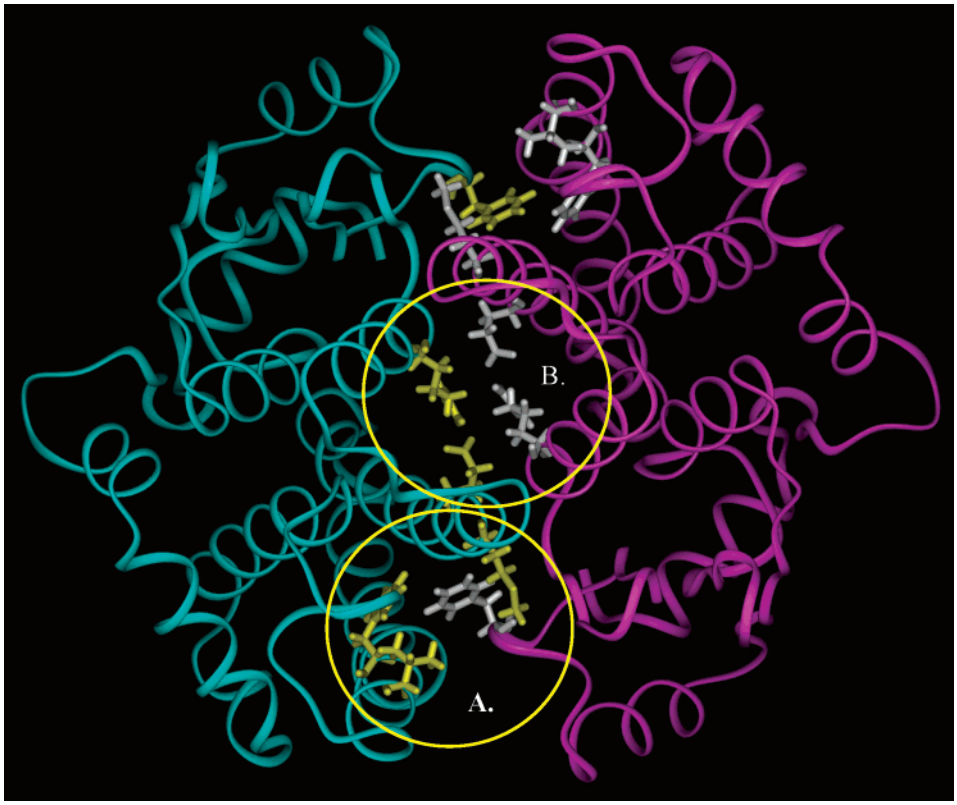

FIGURE 1: Model of rat GST 1-1 showing the two regions of the interface within the dimer. Amino acid residues of subunit A (cyan) are in yellow, and amino acid residues of subunit B (pink) are in gray: (A) hydrophobic ball-and-socket region and (B) ionic Arg/Glu region.

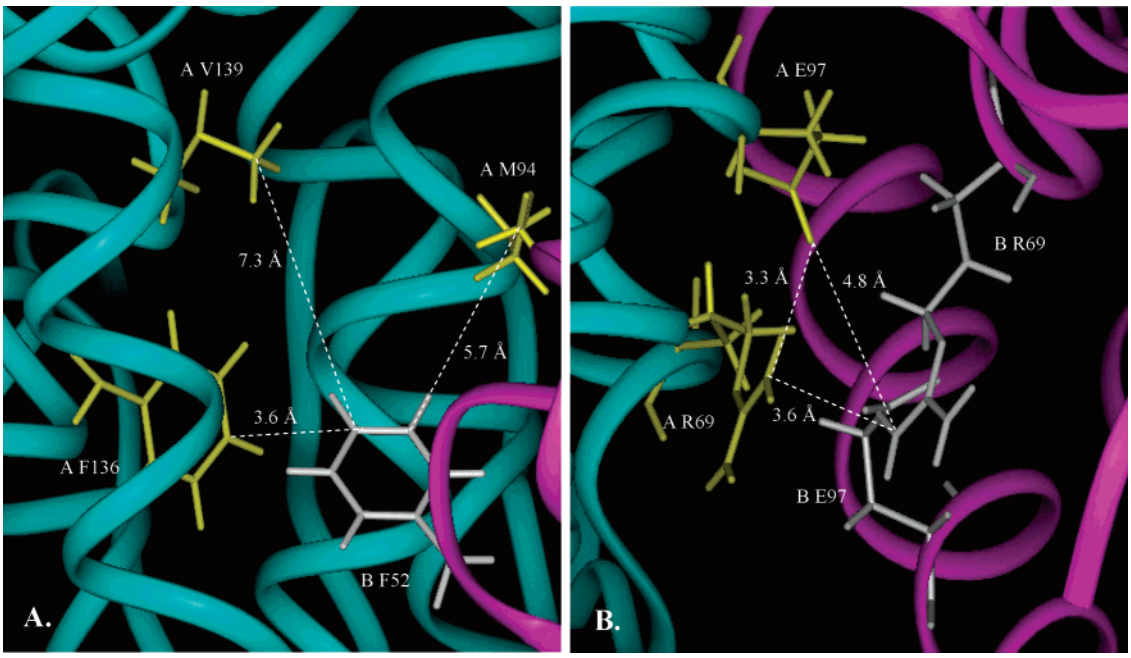

FIGURE 2: Model of rat GST 1-1 showing the regions of the interface that were studied. Subunit A is in cyan, and amino acid side chains of this subunit are in yellow. Subunit B is in pink, and amino acid side chains of this subunit are in gray. (A) Region 1 (hydrophobic ball and socket). Residues which were mutated are displayed along with the distance to the closest atom on Phe52. (B) Region 2 [ionic interaction (Arg/Glu region)]. Residues 97 and 69 from both subunits are displayed along with the closest distance between them.

opposite subunit (Figure 2A). The second interface region (Figure 1B) that we studied is a region involving ionic interactions in which the guanidino group of an arginine interacts with the carboxylate group of a glutamate residue. This region is formed by Arg69 and Glu97 from both subunits interacting at the interface (Figure 2B). Arg69 forms a salt link with Glu97 (3.3 Å apart) of the same monomer; the distance between the Arg and Glu of opposite subunits is 4.8 Å, and the guanidino groups of the two arginines are 3.6 Å apart. We mutated these residues to evaluate which amino acids of the subunit interface make the most important interactions and which alternate amino acids could be

substituted. The activities of the enzymes were studied along with the resulting molecular masses to determine if monomers could be produced by introducing single mutations and whether the monomers exhibit activity. A preliminary version of this work has been published (*11*).

MATERIALS AND METHODS

Reagents. Glutathione (GSH) and 1-chloro-2,4-dinitrobenzene (CDNB) were purchased from Sigma. Ni−NTA resin was purchased from Qiagen. Oligonucleotides for mutagenesis were purchased from Biosynthesis, Inc., and primers for DNA sequencing were purchased from LiCor, Inc., or Biosynthesis, Inc. Bio-Rad dye reagent concentrate was purchased from Bio-Rad Laboratories.

Plasmids and Mutagenesis. The full-length cDNA for rat glutathione *S*-transferase 1-1 was encoded in a pKK2.7 plasmid, as described by Wang *et al*. (*12*) and Dietze *et al*. (*13*), and was a gift from W. M. Atkins at the University of Washington (Seattle, WA). Site-directed mutagenesis was performed using the Stratagene QuikChange kit. The following oligonucleotides and their complements were used to incorporate the mutations (position of the mutation underlined): F52A, GAC GGG AAT TTG ATG GCT GAC CAA GTG CCC; F52Y, GAC GGG AAT TTG ATG TAT GAC CAA GTG CCC; F136A, CGG TAC TTG CCT GCC GCT GAA AAG GTG TTG; F136Y, CGG TAC TTG CCT GCC TAT GAA AAG GTG TTG; F136Q, CGG TAC TTG CCT GCC CAG GAA AAG GTG TTG; M94A, G AGA GCC CTG ATT GAC GCG TAT TCA GAG GG; V139A, GCC TTT GAA AAG GCG TTG AAG AGC CAT GGC; R69E, G CTG GCA CAG ACC GAA GCC ATT CTC AAC; R69Q, G CTG GCA CAG ACC CAA GCC ATT CTC AAC; and E97Q, GCC CTG ATT GAC ATG TAT TCA CAG GGT ATT TTA GAT CTG. Two double mutants were also constructed (R69Q/F136A and R69Q/M94A). One mutation was made, and then, using the cDNA encoding the single mutant enzyme, the second mutation was introduced by site-directed mutagenesis. Mutations were confirmed by DNA sequencing (forward sequencing primer, 5′-GTT GAC AAT TAA TCA TCG GC; and reverse sequencing primer, 5′-ATC AGA CCG CTT CTG CGT TC) which was carried out at the University of Delaware Biology Core Facility using a Long Readir 4200 DNA sequencer from LiCor, Inc., or at the Delaware Biotechnology Institute and University of Delaware Center for Agricultural Biotechnology using an ABI Prism model 377 DNA sequencer (PE Biosystems).

Incorporation of a Six-His Tag. A six-histidine tag was incorporated at the N-terminus of the protein. The His tag was incorporated using a PCR technique based on a procedure in the QIA expressionist handbook from Qiagen. A forward primer (a 52-mer) was used which incorporates the six histidines (after the initiator methionine) and the 5′-restriction site (*Eco*RI) (forward primer, 5′-CAG GAA ACA GAA TTC ATG CAT CAC CAT CAC CAT CAC TCT GGG AAG CCA GTG C) and a reverse primer (a 20-mer) which incorporates the 3′-restriction site (*Hin*dIII) (reverse primer, 5′-CCA AGC TTG GCT GCA GGT CG). These primers were used to amplify the wild-type GST insert. The new GST 1-1 insert, with the His tag, was digested with *Hin*dIII and *Eco*RI. The insert was then ligated into the original plasmid (digested with *Hin*dIII and *Eco*RI) using T4 DNA ligase. The six-His tag has no effect on the activity of the enzyme.

Protein Purification. GST 1-1 was expressed in JM105 *Escherichia coli*. Cells were grown at 37 °C, and when the A_{600} reached 0.4, the cells were induced with 1 mM IPTG. After induction, the cells were grown at 25 °C for 24 h, at which time they were harvested by centrifugation at 10000*g* for 20 min. The pellets were then frozen at −80 °C. Cells were resuspended in 10 mM Tris (pH 7.8, approximately 50 mL for 6 L of culture), followed by sonication for 6 min using a sonicator (Ultrasonic, Inc.) at 20 kHz and 475 W. This suspension was then centrifuged for 25 min at 10000*g*. For mutants with a His tag (R69E, R69Q, E97Q, F136Q, R69Q/F136A, and R69Q/M94A), the enzyme activity in the supernatant was assayed and applied to a Ni−NTA column (∼7 mL of resin) equilibrated with 10 mM Tris buffer (pH 7.8 and 4 °C). The column was washed first with 10 mM Tris (pH 7.8) followed by 10 mM Tris buffer (pH 7.8) containing 0.2 M NaCl. The enzyme was eluted using a linear gradient of imidazole (from 0 to 0.5 M) in 10 mM Tris buffer (pH 7.8) containing 0.2 M NaCl (100 mL of each buffer). The fractions exhibiting activity were pooled and dialyzed into 0.1 M KPO_4 buffer (pH 6.5) containing 1 mM EDTA. The protein concentration was determined using an ϵ_{270} of 22 000 M^{-1} cm^{-1} (*14*) and an M_r of 25 500 per subunit (*2*). Some mutant enzymes did not have the six-His tag (F52A, F52Y, F136A, F136Y, F136E, V139A, and M94A) and, therefore, were purified using affinity chromatography on *S*-hexylglutathione agarose as previously described (*15*). Briefly, the column was eluted with 10 mM Tris buffer (pH 7.8) followed by 10 mM Tris buffer (pH 7.8) containing 0.2 M NaCl, to elute any weakly bound proteins. The GST was eluted with 10 mM Tris buffer (pH 7.8) containing 0.2 M NaCl and 2.5 mM *S*-hexylglutathione and dialyzed into 0.1 M KPO_4 buffer (pH 6.5) containing 1 mM EDTA. The purity of the enzymes was determined using SDS−PAGE or N-terminal sequencing, performed on an Applied Biosystems Procise Sequencing System.

Enzymatic Assays. Enzyme activity was measured using a Hewlett-Packard 8453 UV−vis spectrophotometer. As a standard assay, the formation of the conjugate of glutathione (GSH) (2.5 mM in assay) and 1-chloro-2,4-dinitrobenzene (CDNB) (1 mM in assay) was monitored at 340 nm ($\Delta\epsilon$ = 9.6 mM^{-1} cm^{-1}) in 0.1 M KPO_4 buffer (pH 6.5), according to the method of Habig *et al*. (*16*).

To determine the K_m for GSH, a range of GSH concentrations was used (generally, 0.02−15 mM) and the CDNB concentration was held constant at 2.5 mM. Similarly, to determine the K_m for CDNB, a range of CDNB concentrations was used (25−4000 μM), while the GSH concentration was held constant at 3 mM. In cases where the GSH K_m is high (e.g., F52A), a constant GSH concentration of 100 mM was used for the determination of K_m for CDNB. V_{max} and the standard error were calculated from an extrapolation of the CDNB data using Sigmaplot.

Circular Dichroism Spectroscopy. Circular dichroism spectroscopy was performed on a Jasco J-710 spectropolarimeter. Ellipticity was measured as a function of wavelength using 0.1 nm increments from 250 to 200 nm. All enzyme samples were ∼0.1 mg/mL in 0.1 M KPO_4 and 1 mM EDTA (pH 6.5). Each scan was repeated five times and averaged, after which the contribution from buffer was subtracted from

each spectrum. The final spectra are represented as the mean molar ellipticity [θ] (degrees per square centimeter per decimole) using the equation $[\theta] = \theta/10nCl$, where θ is the measured ellipticity in millidegrees, l is the cell path length in centimeters, C is the molar concentration of protein subunits, and n is the number of residues per subunit. The protein concentration was determined using the Bio-Rad protein assay, based on the Bradford method (*17*), using a Bio-Rad 2550 RIA plate reader with a 600 nm filter. Wild-type GST 1-1 was used as the protein standard.

Determination of the Molecular Mass of the Enzymes. Several methods were used to determine the molecular masses of the enzymes: light scattering, native polyacrylamide gel electrophoresis, and/or analytical ultracentrifugation. Light scattering was performed using a miniDAWN laser photometer from Wyatt Technology. All samples (0.05−0.3 mg/mL) were in 0.1 M KPO_4 and 1 mM EDTA (pH 6.5) and filtered through a 0.02 μm filter before being used. Data were collected using ASTRA for Windows. The protein concentration was determined using the Bio-Rad protein assay (*17*).

Native polyacrylamide gel electrophoresis was used in the case of F52A to determine the oligomeric state. The gel compositions were 20 mM KPO_4 (pH 6.0) 0.12% *N,N,N′,N′*-tetramethylethylenediamine, 0.2 mg/mL ammonium persulfate, and appropriate volumes of distilled water and a 37.5:1 acrylamide/bisacrylamide mixture to form the desired percent acrylamide gels. A range of acrylamide gels were run (7−12%), and the molecular mass was determined using the method of Hedrick and Smith (*18*).

Analytical ultracentrifugation was used to measure molecular masses for wild-type, R69E, R69Q, F136Q, and F52A enzymes, and to determine K_d values for enzyme samples. Using a Beckman Optima XL-A analytical ultracentrifuge, sedimentation equilibrium experiments were performed at 15 000, 17 000, and 20 000 rpm using an An-60 Ti rotor running at a temperature of 10 °C. The samples (0.02−0.33 mg/mL) in 0.1 M KPO_4 and 1 mM EDTA (pH 6.5) were centrifuged until equilibrium was reached (~24 h), at which time data were collected at 280 or 220 nm (equilibrium was confirmed by scanning at 5 h intervals). The activity was determined before and after the entire run to be sure that the protein was stable over the time period. Stepwise radial scans were performed at the particular wavelength, using a step size of 0.001 cm. The resulting data were fit globally using IgorPro (Wavemetrics, Inc.) as previously described in refs *19* and *20*. For samples run in the presence of GSH (2.5 mM), data were collected at 235 and 240 nm because of the sizable contribution of GSH to the absorbance at 220 nm. The dissociation constant (K_d) for dissociation of the dimer to the monomer was calculated using IgorPro in which the monomer molecular mass is entered along with the extinction coefficient.

Molecular Modeling and Insight. Molecular modeling was conducted using the Insight II modeling package from Molecular Simulations, Inc., on an Indigo 2 workstation from Silicon Graphics. The model of rat GST 1-1 was constructed as previously described (*15*) based on the known crystal structure of human GST 1-1 (PDB entry 1GUH). The amino acid sequences of human and rat GST 1-1 are 76% identical and 11% similar, and therefore, the structure of the human enzyme provides a good basis for constructing the rat homology model. This homology model was used to produce the Insight figures and measure the distances between amino acid side chains at the subunit interface.

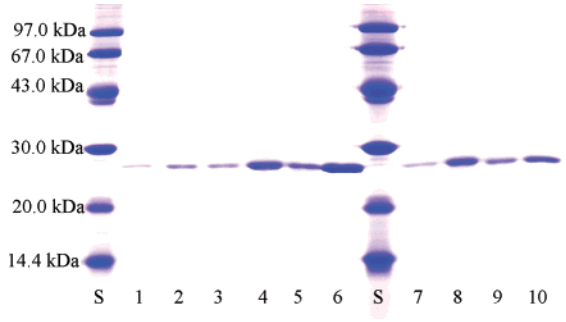

FIGURE 3: SDS−PAGE of representative purified enzymes: lane S, protein standards; lane 1, wild type; lane 2, M94A; lane 3, V139A; lane 4, F136Y; lane 5, F52Y; lane 6, E97Q; lane 7, F136A; lane 8, F52A; lane 9, R69Q; and lane 10, R69E. The standards are 94, 67, 43, 30, 20, and 14.4 kDa.

RESULTS

Expression and Purification. Mutations made to the "ball-and-socket region" of glutathione *S*-transferase were constructed, and the resultant proteins were expressed and purified. Met94, Val139, Phe136, and Phe52 were each mutated to Ala. In addition, Phe52 was replaced with Tyr and Phe136 with Glu, Gln, and Tyr. The plasmids were transformed into *E. coli*, and the cells were grown and induced for expression. These mutant enzymes were purified using an *S*-hexylglutathione agarose affinity column. All enzymes were eluted using buffer containing 2.5 mM *S*-hexylglutathione, except for F52A, which was eluted earlier, predominantly with 10 mM Tris buffer (pH 7.8) containing 0.2 M NaCl. The behavior of F52A is probably a result of the decreased affinity of F52A for GSH.

Arg69 and Glu97 are in the second region of the interface. Mutations of Arg69 to Glu and Gln (containing the His tag) were introduced and overexpressed, and the enzymes were purified. Mutation of Glu97 to Gln (containing the His tag) was also carried out. These mutant enzymes were purified using a Ni−NTA column. All enzymes were purified to homogeneity, yielding a single band by SDS−PAGE (representative enzymes shown in Figure 3). N-Terminal protein sequencing of each purified GST also indicated the presence of one protein (N-terminal sequence of SGKPVLHYFNARGRM and N-terminal sequence of MHHHHHHSGKPVLHY for the proteins with the His tag).

Kinetic Parameters for Enzymes with Subunit Interface Mutations. The results of steady-state kinetics measurements for enzymes with replacements of amino acids in the ball-and-socket region are shown in Table 1. The K_m for GSH does not change appreciably for any of the enzymes with mutations of the socket residues. In contrast, when the ball residue, Phe52, is replaced with Ala, the K_m for GSH increases drastically (~50-fold). The K_m for CDNB also does not change appreciably for any of the mutations of the socket residues. However, there is a 2-fold increase in the K_m for F136A and F136Q; we consider this to be a relatively small effect. The V_{max} values, as determined from an extrapolation of the CDNB kinetic data using Sigmaplot, do not change appreciably for the socket residues. The greatest change in V_{max} is seen in that of F136A, which is reduced to 30% of

Table 1: Glutathione and CDNB Kinetics for Wild-Type and Mutant Enzymes of the Ball-and-Socket Region

enzyme	K_m(GSH) (mM)	K_m(CDNB) (mM)	V_{max}[a] (μmol min^{-1} mg^{-1})
wild type	0.24 ± 0.02	0.54 ± 0.03	52.8 ± 3.0
F52A	10.1 ± 1.3	1.94 ± 0.56	3.7 ± 0.6
F52Y	0.26 ± 0.03	0.35 ± 0.06	43.5 ± 1.6
V139A	0.19 ± 0.02	0.52 ± 0.06	39.2 ± 1.4
M94A	0.22 ± 0.02	0.75 ± 0.09	44.1 ± 2.1
F136A	0.36 ± 0.02	1.16 ± 0.18	15.3 ± 2.3
F136Y	0.16 ± 0.01	0.33 ± 0.04	58.6 ± 2.2
F136Q	0.27 ± 0.02	1.23 ± 0.16	34.1 ± 2.2
F136E	0.22 ± 0.06	0.67 ± 0.14	24.1 ± 1.2

[a] V_{max} and the standard error were determined from an extrapolation to infinite concentrations of the CDNB kinetic data using Sigmaplot.

Table 2: Glutathione and CDNB Kinetics for Wild-Type and Mutant Enzymes of the Arg/Glu Region

enzyme	K_m(GSH) (mM)	K_m(CDNB) (mM)	V_{max}[a] (μmol min^{-1} mg^{-1})
wild type-His	0.20 ± 0.03	0.67 ± 0.04	52.8 ± 3.0
R69Q-His	0.63 ± 0.07	0.53 ± 0.04	23.8 ± 0.6
R69E-His	0.70 ± 0.09	0.88 ± 0.18	12.5 ± 0.8
E97Q-His	0.34 ± 0.03	0.50 ± 0.05	42.6 ± 1.1

[a] V_{max} and the standard error were determined from an extrapolation to infinite concentrations of the CDNB kinetic data using Sigmaplot.

that of the wild type. In the case of F52A, the K_m for CDNB increases by a factor of 4 and the V_{max} is drastically decreased to less than 10% of that of the wild type. On the basis of these results, the most important residue in this region appears to be Phe52.

The results of steady-state kinetic measurements for enzymes with replacements at the Arg/Glu region are given in Table 2. There are no major changes in the K_m values for GSH; however, there is a small, but significant, increase for R69Q and R69E. For the CDNB K_m, the results do not change appreciably from those of the wild type. The greatest change in V_{max} for these mutant enzymes is for R69E, the V_{max} of which is ~24% of that of the wild type. These results suggest that Arg69 is an important residue in this region because either eliminating or reversing the charge results in a decreased V_{max} and an increased K_m for GSH.

Circular Dichroism Spectroscopy for Wild-Type and Mutant Enzymes. CD spectra for all the mutants and the wild type were recorded to evaluate whether the mutations caused changes in the secondary structure of the enzyme. The CD spectra of all of the mutants are very similar to that of the wild type, with the exception of the spectrum of F52A which appears to have a flatter curve in the range of 208−210 nm than do the other spectra (Figure 4A−C). The results indicate that the mutations do not cause major changes in the secondary structure of the enzymes.

Determination of Molecular Masses. Molecular masses for most ball-and-socket mutant enzymes were determined using light scattering (Table 3). Each sample was measured over a range of protein concentrations (usually 0.05−0.2 mg/mL). The weight average molecular masses for all enzymes with mutations of socket residues are very close to the wild-type molecular mass. The largest change in the average molecular mass was observed for the F52A enzyme. This lower average mass (42 kDa) was confirmed by native polyacrylamide gel electrophoresis (39 kDa) (Figure 5) and analytical ultracentrifugation (32 kDa). On the basis of analytical ultracentrifugation, the K_d for dimer dissociation of F52A is higher than that for the wild type (Table 5). Representative data from the analytical ultracentrifuge are given in Figure 6 (wild-type enzyme at 0.3 mg/mL). When Phe52 is replaced with Ala, the equilibrium between the dimer and monomer shifts toward the monomer.

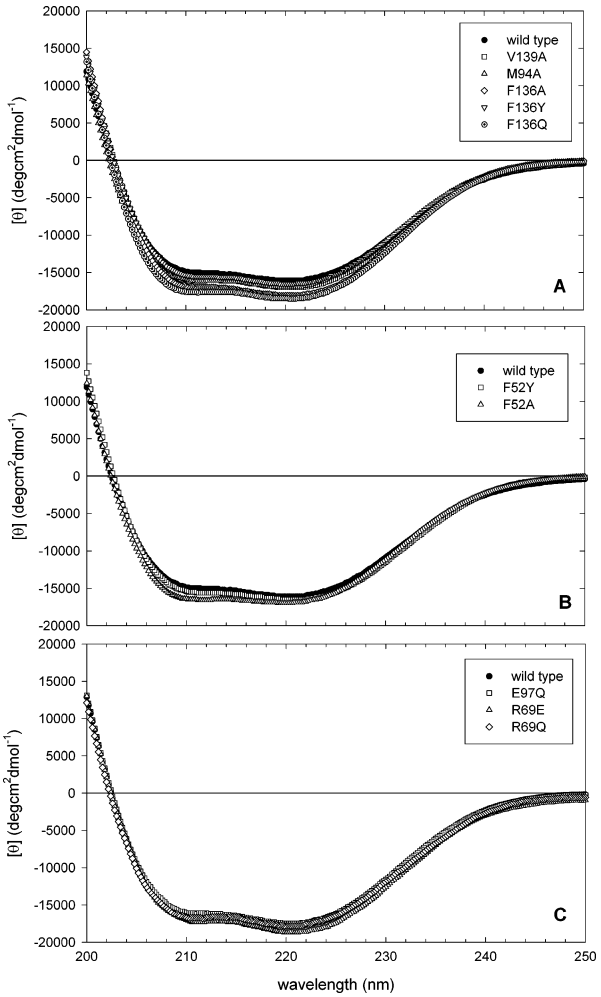

FIGURE 4: Circular dichroism spectra for wild-type and mutant glutathione *S*-transferases. Each spectrum is corrected for the background contributed by buffer and is expressed as [θ]. (A) Wild type and enzymes with mutations in the socket region: wild type (●), V139A (□), M94A (△), F136A (◇), F136Y (▽), and F136Q (⊕). (B) CD spectra for the wild type and enzymes with mutations in the ball region: wild type (●), F52Y (□), and F52A (△). (C) CD spectra for the wild type and enzymes with mutations in the Arg/Glu region: wild type (●), E97Q (□), R69E (△), and R69Q (◇).

Table 3: Weight Average Molecular Masses As Determined by Light Scattering in the Ball-and-Socket Region for Wild-Type and Mutant Enzymes

enzyme[a]	molecular mass (kDa)	enzyme[a]	molecular mass (kDa)
wild type[b]	52 ± 4	M94A	56 ± 2
F52A[b]	42 ± 4	F136A	53 ± 2
F52Y	46 ± 3	F136Y	51 ± 2
V139A	46 ± 2	F136E	55 ± 1

[a] Concentration range of 0.05−0.3 mg/mL. [b] Also determined using native gel electrophoresis: 47 kDa for the wild type and 39 kDa for F52A.

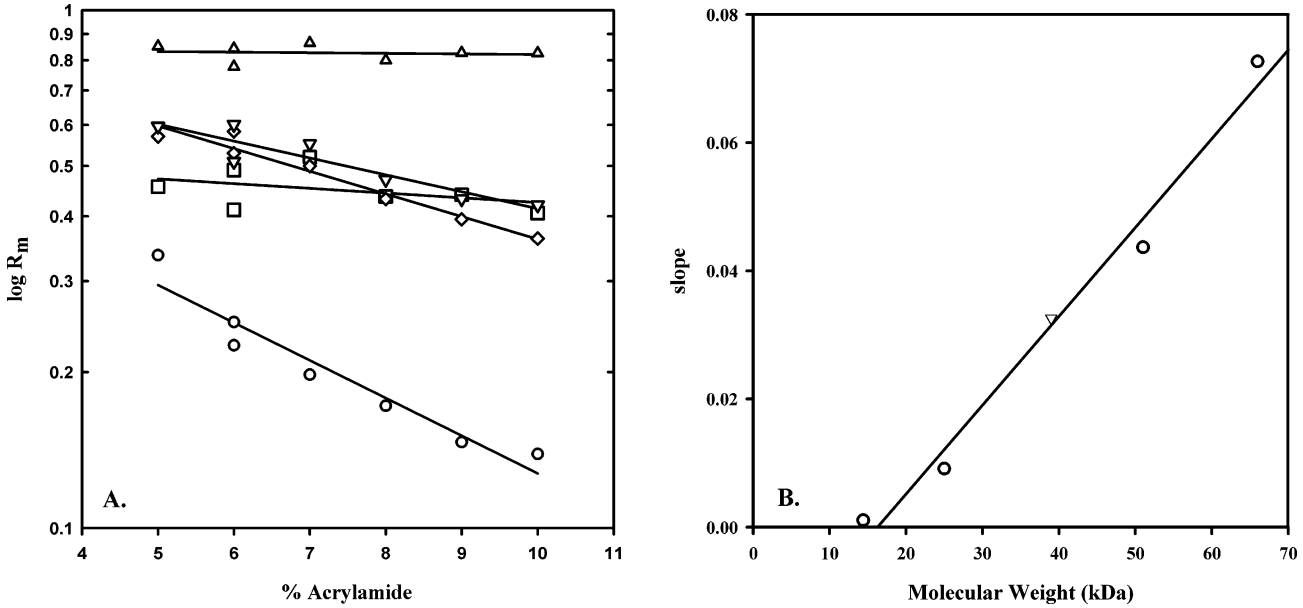

FIGURE 5: Native polyacrylamide gel electrophoresis data for F52A. (A) Plot of log R_m vs % acrylamide: lysozyme, 14.4 kDa (△); chymotrypsinogen, 25 kDa (□); wild-type GST A1-1, 51 kDa (◇); phosphoglycerate mutase, 66 kDa (○); and F52A (▽). (B) Plot of slope vs molecular mass (kilodaltons). The slope for each protein is determined from the line in panel A and then plotted against its molecular mass. The molecular mass determined for F52A is 39 kDa (designated by ▽).

Table 4: Weight Average Molecular Masses As Determined by Light Scattering in the Arg/Glu Region for Wild-Type and Mutant Enzymes

enzyme[a]	molecular mass (kDa)	enzyme[a]	molecular mass (kDa)
wild type-His	52 ± 4	E97Q-His	48 ± 4
R69Q-His	42 ± 2	R69Q/F136A-His	37 ± 4
R69E-His	38 ± 3	R69Q/M94A-His	34 ± 4

[a] Concentration range of 0.05−0.3 mg/mL.

Table 5: Sedimentation Equilibrium Data and the Corresponding K_d Values

initial concentration (mg/mL)	wavelength (nm)	weight average molecular mass (kDa)	K_d (μM)
		Wild Type-His	
0.37	280	50.5 ± 0.1	0.34 ± 0.07
0.06	220	47.1 ± 0.2	
		R69Q-His	
0.28	280	48.6 ± 0.2	0.92 ± 0.14
0.06	220	41.3 ± 0.9	
		R69E-His	
0.31	280	46.2 ± 0.1	3.4 ± 0.9
0.07	220	33.3 ± 0.9	
0.04	220	34.2 ± 1.3	
		F52A	
0.04	220	31.9 ± 2.4	3.1 ± 1.0
		F136Q	
0.04	220	48.1 ± 2.2	0.08 ± 0.04

For the Arg/Glu region, the molecular mass was determined by both light scattering (Table 4) and analytical ultracentrifugation (Table 5). A dissociation constant (K_d) for dissociation of the dimer to the monomer (molecular mass of 26.4 kDa with the His tag) was determined directly from the analytical ultracentrifugation data. Although the weight average molecular masses depend on the protein concentration, the K_d remains constant. The most striking change occurs when the charge of Arg69 is reversed. R69E has a

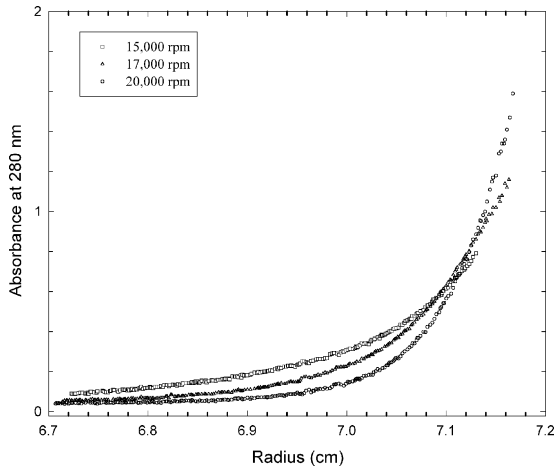

FIGURE 6: Sedimentation equilibrium data using the wild-type enzyme at 0.33 mg/mL and monitoring at 280 nm. The data are shown for three speeds: 15 000 (□), 17 000 (△), and 20 000 rpm (○). The data are fit globally to the equation $c_r = [c_0 e^{(\omega^2 M/2RT)(1-\nu\rho)(r^2-r_0^2)}] + E$, where c_r is the concentration at any given radius (r), c_o is the concentration of the monomer at the reference radius r_0, ω is the angular velocity, M is the monomer molecular mass of the species (26.4 kDa for GST A1-1), ν is the partial specific volume of the solute (0.7425 for GST 1-1), and ρ is the density of the solvent (1.0013 in this case), using IgorPro.

weight average molecular mass much closer to that of the monomer. The corresponding K_d values also show that the equilibrium of the monomer and dimer has shifted toward the monomer for this particular mutant.

The molecular masses for the double mutants R69Q/F136A and R69Q/M94A (Table 4) were determined using light scattering. The molecular masses were lower for the double mutants than for any of these single mutants.

For those single mutants with lower average molecular masses, the effect of the addition of GSH was tested using analytical ultracentrifugation (Table 6). The addition of a substrate better mimics the conditions of the assay. Furthermore, two residues (Asp101 and Arg131) which contribute

Table 6: Sedimentation Equilibrium Data for Enzymes in the Presence of 2.5 mM GSH[a]

initial concentration (mg/mL)	weight average molecular mass (kDa)	K_d (μM)
	Wild Type-His	
0.06	50.1 ± 0.3	0.05 ± 0.02
	R69Q-His	
0.04	47.8 ± 1.2	0.08 ± 0.02
	R69E-His	
0.06	44.1 ± 1.0	0.9 ± 0.2
0.04	43.1 ± 3.0	
	F52A	
0.04	38.0 ± 2.8	1.1 ± 0.9

[a] Data taken at 235 nm due to the contribution of GSH to the absorbance at 220 nm.

contacts to the GSH come from the other subunit, and therefore, glutathione might be expected to stabilize the dimer. For all mutants except F52A, the addition of GSH results in a weight average molecular mass much closer to the dimer molecular mass. In the case of F52A, the weight average molecular mass does exhibit a slight increase with the addition of GSH, but the magnitude of the increase is not as great as is seen for the other mutant enzymes. K_d values were calculated in the absence and presence of GSH to quantitate the effect of substrate on the weight average molecular mass. As expected, the mutants with the lower weight average molecular masses have higher K_d values. The increase in the weight average molecular mass upon addition of GSH is consistent with preferential binding of glutathione to the dimer.

DISCUSSION

We have made single replacements for amino acids in two regions of the subunit interface of glutathione *S*-transferase A1-1 and studied the protein molecular masses using light scattering and analytical ultracentrifugation. None of the substitutions made for socket amino acids changed the weight average molecular mass. When the ball residue was mutated from Phe to another large, bulky aromatic residue such as Tyr, the weight average molecular mass was also found to be characteristic of a dimer. However, when the ball residue was changed to a small residue such as Ala, the weight average molecular mass was reduced and the equilibrium shifted toward the monomer. In a previous study, Tyr50 of human GSTpi was mutated, which is the residue corresponding to Phe52 of rat GSTA1-1. Tyr was mutated to Ala, Arg, Phe, Leu, and Thr (*21*). To determine the molecular masses, size-exclusion chromatography was used, and in all cases, the mutant enzymes were reported to be dimers. However, no data were shown, and because there is a protein concentration dependence of molecular mass, the concentration at which these experiments were conducted is important.

In this study, for the Arg/Glu region, eliminating the charge did not cause a marked shift in the weight average molecular masses. In contrast, when the charge was reversed at position 69, the weight average molecular mass of R69E was greatly decreased toward that of the monomer. Replacement of arginine with glutamate results in four negative charges in the region and thus considerable electrostatic repulsion, causing a higher K_d. On the basis of these results, the most important residues contributing to dimer stability are Phe52 and Arg69. In addition, when mutations from each region are combined, the weight average molecular mass is lower than that of the individual mutations, indicating the cumulative effect of these amino acids in stabilizing the enzyme dimer. There have been other systems in which single or double mutations at the interface result in monomers or a shifted equilibrium, e.g., aldolase A (*22*), alkaline phosphatase (*23*), phosphoribosylanthranilate isomerase (*24*), and Cu,Zn superoxide dismutase (*25*).

The activity of the mutant GSTs M94A and V139A shows no great change in K_m for GSH or CDNB or V_{max}, as compared to those of the wild type. These socket residues do not make any close contacts with either the glutathione or CDNB binding sites; the shortest distance to the enzyme-bound glutathione from its own subunit is ~17 Å. Therefore, it was not surprising that there are no drastic changes in the kinetic constants. When the aromatic interaction between Phe136 and Phe52 was retained in F136Y, there was no appreciable change in V_{max} or K_m; however, replacement of Phe136 with Ala yields a longer distance between F136A and Phe52, resulting in a lower V_{max} and a slightly increased K_m for CDNB. When Phe52 was replaced with tyrosine, the kinetic characteristics of the mutant enzyme were close to those of the wild type. This result was not surprising, because there are other isozymes of glutathione *S*-transferases with Tyr at this position [e.g., the human pi isozyme (*26*)]. However, when Ala was introduced in place of Phe52, the kinetic constants changed drastically: the K_m for GSH is 50 times that of the wild type, and the V_{max} is very low (less than 10% of that of the wild type). This lower activity is similar to that of an F51S mutant of human GST A1-1 (*27*). Phe52 is located on a loop which connects α-helix 2 and β-strand 3 in domain I of the subunit. When the *S*-benzylglutathione binds in its extended conformation, it runs antiparallel to the loop connecting α-helix 2 and β-strand 3 (Figure 7A) (*10*). There are several residues in this region which make contact with the glutathione. The side chain of Lys45 makes an electrostatic interaction with the carboxy terminus of the GSH, and the main chain carbonyl and amide nitrogen of Val55 make hydrogen bonds between the amide nitrogen and main chain carbonyl of the cysteine moiety of GSH (Figure 7A). The F52A mutation most likely causes a local conformational change in the area of the loop, which in turn causes small shifts in α-helix 2 and β-strand 3 lining the GSH binding site, resulting in a high K_m. In addition, there are two amino acids from the opposite subunit that make contact with GSH, thereby contributing to the affinity of the substrate for the enzyme. The negatively charged Asp101 interacts with the positively charged α-amino group of glutathione, and the positively charged Arg131 interacts with the negatively charged carboxylate of the glycine moiety of the glutathione. A shift in the monomer−dimer equilibrium toward the monomer may affect the binding of GSH because the stabilizing contacts to GSH from the other monomer are not present. Phe52 appears to be very important for both activity and maintaining the correct structure in the region for GSH binding.

There are no appreciable changes in the kinetics for the E97Q mutant. Glu97 is far from the substrate binding sites; the shortest distance is ~8 Å between it and the GSH binding site of the opposite subunit. However, the Arg69 mutations

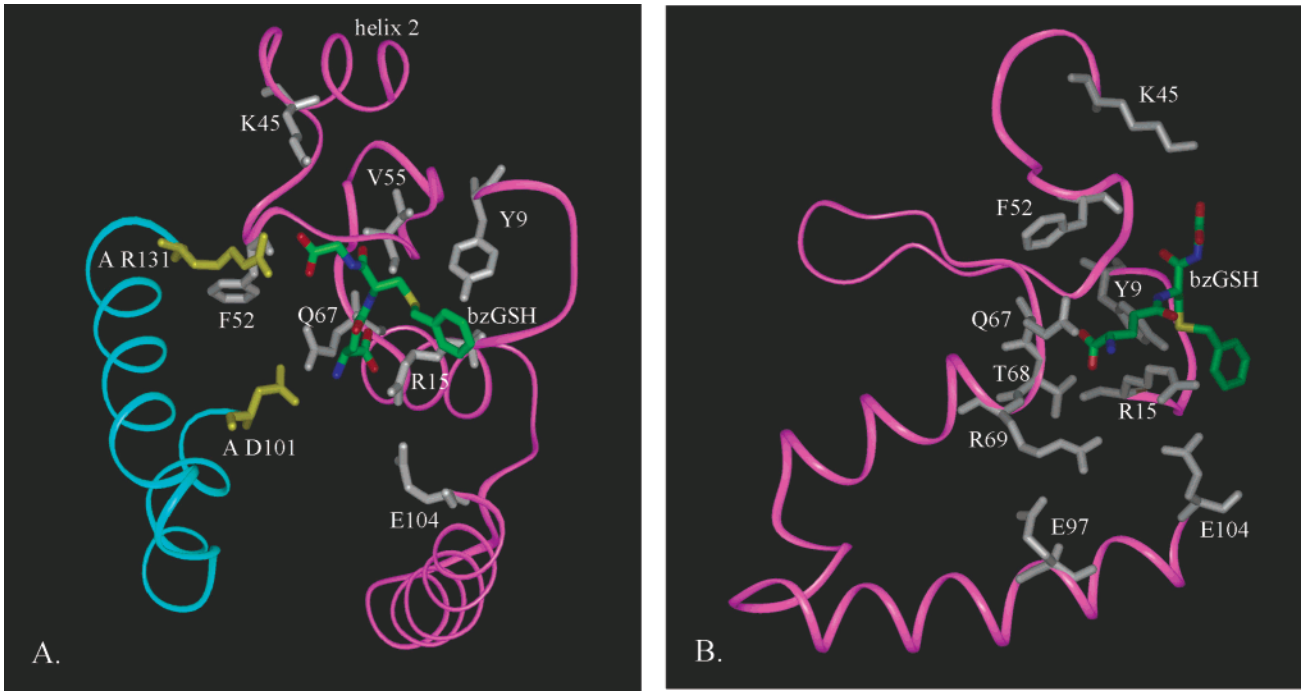

FIGURE 7: Model of rat GST 1-1 showing the relationship between the regions of the subunit interface and the glutathione site. *S*-Benzylglutathione (colored by atom) is shown bound in the active site. Subunit A is in cyan, and amino acid side chains of this subunit are in yellow. Subunit B is in pink, and amino acid side chains of this subunit are in gray. (A) Phe52 and its relationship to the glutathione site of the same subunit. (B) Arg69 and Glu97 and the relationship to the glutathione site of the same subunit.

(R69Q and R69E) do change the K_m for GSH significantly, and the V_{max} is decreased. Arg69 is a neighbor of Thr68 and Gln67 (Figure 7B). The side chain of Thr68 and its main chain nitrogen make hydrogen bonds with the carboxylate of the γ-Glu of the GSH, while the side chain carbonyl of Gln67 hydrogen bonds to the amino terminus of GSH. The guanidino group of Arg69 is 5 Å from Glu104, which makes an electrostatic interaction with the positively charged Arg15; Arg15 is unique to the alpha class, and it helps to orient Tyr9 to lower the pK_a of the thiol of GSH. The amide nitrogen of Arg69 is 5 Å from the carbon of the carboxylate group of the γ-Glu. Replacing Arg69 with either Glu or Gln interferes with some of these interactions, thereby causing small changes in the local environment which result in the small but significant increases in the K_m for GSH and the decrease in V_{max}.

GSTs are crystallized as dimers, but our experiments show that in solution wild-type and mutant enzymes undergo reversible association and dissociation, the extent of which depends on protein concentration. Whether the enzyme can exist as a stable monomer and retain activity has not yet been resolved. A monomeric species of a human GSTpi has been constructed by introducing 10 site specific mutations (*28*). This drastically changed enzyme was structurally stable, but retained no activity. In the absence of glutathione, we have found that in the single mutant enzymes, R69E and F52A, the monomer predominates at low protein concentrations.

The literature abounds in examples of recombinant proteins which are expressed in bacteria as fusion proteins with glutathione *S*-transferase. Typically, the construct is made to facilitate purification of the target protein. On the other hand, the dimerization of the GST may cause problems, such as artificially promoting the nonphysiological dimerization of the target protein (*29*−*31*). It is possible that use of a mutant glutathione *S*-transferase (such as the R69E enzyme), which has a greatly weakened tendency to dimerize but retains appreciable activity, would improve certain applications of GST fusion proteins.

The weight average molecular mass in the presence of GSH is shifted toward the dimer for R69E. For F52A, the weight average molecular mass increases only slightly in the presence of GSH. Many contacts to GSH are disrupted by mutating Phe52 to Ala, and therefore, even in the presence of GSH, less dimer is formed in the F52A enzyme.

The amount of monomer present under assay conditions can be calculated using the K_d determined in the presence of GSH and the protein concentration (in terms of subunits) at which the enzyme is assayed. Because R69E has a higher specific activity than F52A, it is assayed at a lower protein concentration. Thus, F52A, under assay conditions, is approximately 50% monomer, while for R69E, there is approximately 90% monomer. In the case of R69E, there is only 10% dimer present in the assay, and even *if we assume that the dimer is completely active*, when we compare the wild-type V_{max} and the V_{max} of R69E (~24% of the wild-type activity), we cannot attribute all of the activity to the dimer that is present. It can be calculated that the specific activity of the monomer is ~8 μmol min^{-1} mg^{-1} or 15% of the specific activity of the dimer. For F52A (with ~7% of that of the wild type), under assay conditions, there is less monomer present because of the high protein concentration (0.03 mg/mL as compared to 0.001 mg/mL for R69E) at which the assay must be carried out. Since the percentage of wild-type activity is *less* than the percentage of dimer present (50%), we cannot conclusively assign the activity to either the monomer or the dimer; however, when the protein is diluted 8-fold, the specific activity does not decrease as the monomer is increased to 93%, suggesting that the monomer and dimer both have very low activity.

This paper demonstrates that Phe52 and Arg69, one in each region of the subunit interface, are important determinants of a stable dimer of glutathione *S*-transferase 1-1. By using single mutations at either position, the equilibrium between the monomer and dimer can be changed. Mutant enzymes F52A and R69E exhibit relatively low weight average molecular masses. From the determined K_d, we have ascertained that for R69E the monomer does in fact retain activity, although its specific activity is lower than that of the dimer. It is possible that mutation of another subunit interface amino acid could perturb the monomer−dimer equilibrium further, while preserving the conformation of the active site. However, the most reasonable conclusion from our results is that for glutathione *S*-transferase A1-1, the monomer has partial activity but the dimeric species is needed for high specific activity.

ACKNOWLEDGMENT

We thank Dr. Joel Schneider and Juliana Kretsinger for training on and use of the analytical ultracentrifuge. Also, we thank Dr. Yu Chu Huang for protein sequencing.

REFERENCES

1. Armstrong, R. N. (1997) Structure, catalytic mechanism, and evolution of the glutathione transferases, *Chem. Res. Toxicol. 10*, 2−18.
2. Mannervik, B., and Danielson, U. H. (1988) Glutathione transferases: structure and catalytic activity, *CRC Crit. Rev. Biochem. Mol. Biol. 23*, 283−337.
3. Wilce, M. C. J., and Parker, M. W. (1994) Structure and function of glutathione S-transferases, *Biochim. Biophys. Acta 1205*, 1−18.
4. Pickett, C. B., and Lu, A. L. H. (1989) Glutathione S-transferases: Gene structure, regulation, and biological function, *Annu. Rev. Biochem. 58*, 743−764.
5. Hayes, J. D., and Pulford, D. J. (1995) The glutathione S-transferases supergene family: Regulation of GST and the contribution of the isoenzymes to cancer chemoprotection and drug resistance, *CRC Crit. Rev. Biochem. Mol. Biol. 30*, 445−600.
6. Mannervik, B. (1985) The isoenzymes of glutathione transferase, *Adv. Enzymol. Relat. Areas Mol. Biol. 57*, 357−417.
7. Barycki, J. J., and Colman, R. F. (1997) Identification of the nonsubstrate steroid binding site of rat liver glutathione S-transferase, isozyme 1-1, by the steroid affinity label, 3β-(iodoacetoxy)dehydroisoandrosterone, *Arch. Biochem. Biophys. 345*, 16−31.
8. Vargo, M. A., and Colman, R. F. (2001) Affinity labeling of rat glutathione S-transferase isozyme 1-1 by 17β-iodoacetoxy-estradiol-3-sulfate, *J. Biol. Chem. 276*, 2031−2036.
9. Benson, A. M., Talalay, P., Keen, J. H., and Jakoby, W. B. (1977) Relationship between the soluble glutathione-dependent Δ^5-3-ketosteroid isomerase and the glutathione S-transferases of the liver, *Proc. Natl. Acad. Sci. U.S.A. 74*, 158−162.
10. Sinning, I., Kleywegt, G. J., Cowan, S. W., Reinemer, P., Dirr, H. W., Huber, R., Gilliland, G. L., Armstrong, R. N., Ji, X., Board, P. G., Olin, B., Mannervik, B., and Jones, T. A. (1993) Structure determination and refinement of human alpha class glutathione transferase A1-1, and a comparison with the mu and pi class enzymes, *J. Mol. Biol. 232*, 192−212.
11. Vargo, M. A., Nguyen, L., and Colman, R. F. (2001) Probing subunit interactions of glutathione S-transferase, *Biochemistry 40*, 8624−8625.
12. Wang, R. W., Pickett, C. B., and Lu, A. Y. H. (1989) Expression of a cDNA encoding a rat liver glutathione S-transferase subunit in *Escherichia coli*, *Arch. Biochem. Biophys. 269*, 536−543.
13. Dietze, E. C., Grillo, M. P., Kalhorn, T., Nieslanik, B., Jochleim, C., and Atkins, W. (1998) Thiol ester hydrolysis catalyzed by glutathione S-transferase A1-1, *Biochemistry 37*, 14948−14957.
14. Katusz, R. M., Bono, B., and Colman, R. F. (1992) Affinity labeling of Cys^{111} of glutathione S-transferase, isoenzyme 1-1, by S-(4-bromo-2,3-dioxobutyl)glutathione, *Biochemistry 31*, 8984−8990.
15. Wang, J., Barycki, J. J., and Colman, R. F. (1996) Tyrosine 8 contributes to catalysis but is not required for activity of rat liver glutathione S-transferase, 1-1, *Protein Sci. 5*, 1032−1042.
16. Habig, W. H., Pabst, M. J., and Jakoby, W. B. (1974) Glutathione S-transferases. The first enzymatic step in mercapturic acid formation, *J. Biol. Chem. 249*, 7130−7139.
17. Bradford, M. M. (1976) A rapid sensitive method for the quantitation of microgram quantities of protein utilizing the principle of protein-dye binding, *Anal. Biochem. 72*, 248−254.
18. Hedrick, J. L., and Smith, A. J. (1968) Size and charge isomer separation and estimation of molecular weights of proteins by disc gel electrophoresis, *Arch. Biochem. Biophys. 126*, 155−164.
19. Kretsinger, J., and Schneider, J. P. (2003) Design and application of basic amino acid displaying enhanced hydrophobicity, *J. Am. Chem. Soc. 125*, 7907−7913.
20. Schneider, J. P., Lear, J. D., and DeGrado, W. F. (1997) A designed buried salt bridge in a heterodimeric coiled coil, *J. Am. Chem. Soc. 119*, 5742−5743.
21. Stenberg, G., Abdalla, A.-M., and Mannervik, B. (2000) Tyrosine 50 at the subunit interface of dimeric human glutathione transferase P1-1 is a structural key residue for modulating protein stability and catalytic function, *Biochem. Biophys. Res. Commun. 271*, 59−63.
22. Beernink, P., and Tolan, D. (1996) Disruption of the aldolase A tetramer into catalytically active monomers, *Proc. Natl. Acad. Sci. U.S.A. 93*, 5374−5379.
23. Boulanger, R., and Kantrowitz, E. (2003) Characterization of a monomeric *E. coli* alkaline phosphatase formed upon a single amino acid substitution, *J. Biol. Chem. 278*, 23497−23501.
24. Thoma, R., Henning, M., Sterner, R., and Kirshner, K. (2000) Structure and function of mutationally generated monomers of dimeric phosphoribosylanthranilate isomerase from *Thermotoga maritima*, *Structure 8*, 265−276.
25. Cioni, P., Stroppolo, C. M., Desideri, A., and Strambini, G. (2001) Dynamic features of the subunit interface of Cu,Zn superoxide dismutase as probed by tryptophan phosphorescence, *Arch. Biochem. Biophys. 391*, 111−118.
26. Reinemer, P., Dirr, H. W., Ladenstein, R., Huber, R., Lo Bello, M., Federici, G., and Parker, M. W. (1992) Three-dimensional structure of class pi glutathione S-transferase from human placenta in complex with S-hexylglutathione at 2.8 Å resolution, *J. Mol. Biol. 227*, 214−226.
27. Sayed, Y., Walllace, L., and Dirr, H. (2000) The hydrophobic lock-and-key intersubunit motif of glutathione transferase A1-1: Implication for catalysis, liganding function and stability, *FEBS Lett. 465*, 169−172.
28. Abdalla, A., Bruns, C., Tainer, J. A., Mannervik, B., and Stenberg, G. (2002) Design of a monomeric human glutathione transferase GSTP1, a structurally stable but catalytically inactive protein, *Protein Eng. 15*, 827−834.
29. Bjorndal, B., Trave, G., Hageborg, I., Lillehaug, J., and Raae, A. (2003) Expression and purification of receptor for activated C-kinase 1 (RACK1), *Protein Expression Purif. 31*, 47−55.
30. Haldeman, M., Xia, G., Kasperek, E., and Pickart, C. (1997) Structure and function of ubiquitin conjugating enzyme E2-25k: The tail is a core-dependent activity element, *Biochemistry 36*, 10526−10537.
31. Niedziela-Majka, A., Rymarczyk, G., Kochman, M., and Ozyhar, A. (1998) Pure bacterially expressed DNA-binding domains of the functional ecdysteroid receptor capable of interacting synergistically with the *hsp* 27 20-hydroxyecdysone response element, *Protein Expression Purif. 14*, 208−220.

BI030245Z